Available at
www.ComputerScienceWeb.com
POWERED BY SCIENCE DIRECT

Signal Processing 83 (2003) 1789–1802

SIGNAL PROCESSING

www.elsevier.com/locate/sigpro

# Low-complexity estimation of 2D DOA for coherently distributed sources

Jooshik Lee[a], Iickho Song[b,*], Hyoungmoon Kwon[a], Sung Ro Lee[c]

[a] *Department of Electrical Engineering, Korea Advanced Institute of Science and Technology, 373-1 Guseong Dong, Yuseong Gu, Daejeon 305-701, South Korea*

[b] *Department of Electrical and Computer Engineering, Queen's University, Kingston, Ont., Canada K7L 3N6*

[c] *Department of Electronics Engineering, Mokpo National University, 61 Dorim Ri, Chunggye Myeon, Muan Gun, Jeonnam 534-729, South Korea*

Received 29 July 2002; received in revised form 19 March 2003

**Abstract**

We consider the estimation of two-dimensional (azimuth and elevation) direction-of-arrival (DOA) using a pair of uniform circular arrays under a coherently distributed source model. Since the coherently distributed source is characterized by four parameters, the nominal azimuth DOA, angular extension of the azimuth DOA, nominal elevation DOA, and angular extension of the elevation DOA, the computational complexity of the parameter estimation is normally highly demanding. We propose a low-complexity estimation algorithm, called the sequential one-dimensional searching algorithm by concentrating only on the estimation of DOAs. The SOS algorithm has a basis on the eigenstructure between the steering matrix and signal subspace, and utilizes preliminary estimates obtained at a pre-processing stage. The SOS algorithm estimates the DOAs, but not the angular extensions: although the SOS algorithm does not provide estimates of angular extensions, it is useful when the angular extensions are small. Specifically, it is shown from simulation results that the SOS algorithm exhibits as good an estimation performance as the maximum likelihoood method for coherently distributed sources.


*Keywords:* Distributed sources; Uniform circular array (UCA); Sequential one-dimensional searching (SOS)

## 1. Introduction

In wireless communications, antenna array processing is considered to be an attractive technique to mitigate such problems as multipath fading and co-channel interference. By employing antenna arrays, the coverage may be improved, co-channel interference reduced, and the capacity increased. To fully achieve these goals, it is necessary to understand and exploit the characteristics of the antenna arrays and the wireless channel [9].

Many signal source localization/estimation with an array of antenna elements has focused on sources that are modeled as points in space. However, in wireless communication environment where multipath dispersion effects exist, a distributed source model may be more appropriate. A number of investigators have proposed distributed source modeling, and several parameter estimation techniques for distributed sources have been proposed in the literature

* Corresponding author.
*E-mail address:* i.song@ieee.org (I. Song).

0165-1684/03/$ - see front matter 
doi:10.1016/S0165-1684(03)00103-8

[1–5,7,8,13–18,20,22,24–27]. For example, the distributed sources have been classified into coherently and incoherently distributed sources [25,20], and attempts for the coherently distributed source modeling and parameter estimation have been accomplished in [25,16], where the signal sources are defined as spatial clusters. The parameters are estimated by some algorithms based on the multiple signal classification (MUSIC) using a uniform linear array (ULA), assuming that the shape of the spatial cluster (that is, the angular weighting function) is identical for all sources.

For the parameter estimation of incoherently distributed sources, a two-step procedure has been proposed in [5] in which decoupling of the estimation of direction-of-arrival (DOA) from that of angular spread is considered by combining a covariance matching algorithm with the extended invariance principle (EXIP). Another approach is proposed in [3], where a rank-two model is fitted to a distributed source and a standard point source DOA algorithm such as the root-MUSIC is used. A parameter estimation algorithm based on the estimation of signal parameters via rotational invariance technique (ESPRIT) for the distributed source model is proposed in [22], where the nominal DOA of the sources is estimated by using the total least square ESPRIT (TLS-ESPRIT) with two closely spaced ULAs and the angular extension is estimated by a one-dimensional distributed source parameter estimator (DSPE) spectrum. The DSPE method provides a low computational complexity for estimating the unknown parameters of distributed sources. Yet, most of the results on distributed source estimation have mainly been developed for azimuth-only estimation of the nominal DOA and angular extension.

Recently, researches based on practical experiment measurements have dealt with parameter estimation using a uniform circular array (UCA) [12,19]. Note that a ULA provides only 180° coverage and is not normally useful for two-dimensional (2D) (azimuth and elevation) DOA estimation while the UCA has 360° azimuthal coverage and provides information on source elevation angles also. In addition, due to the rotational symmetry of the array configuration, the resolution performance of a UCA is independent of the azimuth angles of the incident waves. The problem of estimating unknown parameters of distributed sources using a UCA has been considered in [26], where a low-complexity estimator for unknown parameters is proposed based on a reparametrized version of the distributed source model proposed in [6]. In spite of the major advantages of the UCA, nonetheless, the distributed source model with a UCA geometry has not yet been studied in sufficient depth.

In this paper, we consider the coherently distributed source model and propose a low-complexity DOA estimation method using a pair of UCAs. The coherently distributed source model in this paper is characterized by four parameters: the nominal azimuth DOA, angular extension of the azimuth DOA, nominal elevation DOA, and angular extension of the elevation DOA. In general, the computational complexity of the optimum estimation methods increases dramatically because of the need for a search over a high-dimensional parameter space. Based on the special array geometry and the relation between the signal subspace and steering vector, the low-complexity DOA estimation method proposed in this paper requires only one-dimensional searches for the nominal azimuth DOA and elevation DOA. In essence, the contribution of this paper is the application of the combination of distributed signal modeling, ESPRIT, and alternate minimization in 2D problem as a collective study.

## 2. Distributed source model

We first review the point source model briefly. Assume that a source results in one plane wave arriving at the receiving antenna from specific elevation $\theta$ and azimuth $\phi$, where a spherical coordinate system is used to represent the arrival directions of the incoming plane waves. Then, the point source model with an array of $L$ sensors can be expressed as

$$\mathbf{x}(t) = \mathbf{a}(\theta, \phi)s(t) + \mathbf{n}(t), \tag{1}$$

where $\mathbf{x}(t)$ is the $L \times 1$ received array output vector, $\mathbf{a}(\theta, \phi)$ is the $L \times 1$ array response vector for the point source signal $s(t)$ at $(\theta, \phi)$, and $\mathbf{n}(t)$ is an $L \times 1$ additive noise vector. The noise is assumed to be zero-mean and spatially and temporally white and Gaussian:

$$E\{\mathbf{n}(t)\mathbf{n}^{\mathrm{H}}(t')\} = \sigma^2 \mathbf{I}_L \delta_{tt'} \tag{2}$$

and

$$E\{\mathbf{n}(t)\mathbf{n}^{\mathrm{T}}(t')\} = \mathbf{0}, \quad \forall t, t', \tag{3}$$

where $\sigma^2$ is the noise variance, $\mathbf{I}_k$ denotes the $k \times k$ identity matrix, $k = 1, 2, \ldots$, and $\delta_{tt'}$ is the Kronecker delta function with $\delta_{tt'} = 1$ for $t = t'$ and $\delta_{tt'} = 0$ for $t \neq t'$. We also assume that the signal is uncorrelated with the noise.

Assuming that we have a UCA, the steering vector $\mathbf{a}(\theta, \phi)$ is

$$\mathbf{a}(\theta,\phi) = [\mathrm{e}^{\mathrm{j}\eta \sin\theta\cos(\phi-\gamma_1)}, \mathrm{e}^{\mathrm{j}\eta \sin\theta\cos(\phi-\gamma_2)}, \ldots, \mathrm{e}^{\mathrm{j}\eta \sin\theta\cos(\phi-\gamma_L)}]^{\mathrm{T}}, \quad (4)$$

where $\mathrm{j} = \sqrt{-1}$, $\eta = 2\pi r/\lambda$, and $\gamma_k = 2\pi(k-1)/L$ for $k = 1, 2, \ldots, L$ with $r$ the radius of the UCA and $\lambda$ the wavelength of the arriving wave. One of the requirements on a UCA is that the distance between adjacent array elements should be less than or equal to $0.5\lambda$: in this paper, the radius is taken as $r = \lambda/(4\sin(\pi/L))$ for convenience so that the distance between adjacent array elements is $0.5\lambda$.

Assume a single narrowband point source that contributes with a large number of wavefronts originating from (possibly unresolvable) multi-path reflections near the source and during transmission. If we observe the baseband signals received at the antenna array, it is possible to regard the source just as a spatially distributed cluster: the cluster can be modeled as a distributed source. When the shape (that is, the angular weighting function) of a distributed source does not change temporally and the received signal components from that source at different angles are fully correlated, we call the source a *coherently distributed* source. For a coherently distributed source we can rewrite (1) as

$$\mathbf{x}(t) = \int\int \mathbf{a}(\vartheta,\varphi)\varsigma(\vartheta,\varphi,t)\,\mathrm{d}\vartheta\,\mathrm{d}\varphi + \mathbf{n}(t), \quad (5)$$

where $\varsigma(\vartheta, \varphi, t)$ is a complex, random, angular-temporal signal intensity, and can be expressed as

$$\varsigma(\vartheta,\varphi,t) = s(t)\varrho(\vartheta,\varphi;\mu) \quad (6)$$

under the coherently distributed source assumptions. In (6), $\varrho(\vartheta, \varphi; \mu)$ is a deterministic angular weighting function of $\vartheta$ and $\varphi$ but not of $t$, and is parametrized by the vector $\mu = (\theta, \sigma_\theta, \phi, \sigma_\phi)$ denoting the nominal elevation DOA $\theta$, angular extension $\sigma_\theta$ of the elevation DOA, the nominal azimuth DOA $\phi$, and angular extension $\sigma_\phi$ of the azimuth DOA. The parameter vector $\mu$ characterizes the distributed source together with the angular weighting function $\varrho(\vartheta, \varphi; \mu)$ which shows the angular spreading of the source.

It is reasonable to assume that $\varrho(\vartheta, \varphi; \mu)$ is non-vanishing only around $(\vartheta, \varphi) = (\theta, \phi)$: that is, we practically have

$$\varrho(\vartheta,\varphi;\mu) = 0, \quad \text{for } |\vartheta-\theta| > \varepsilon_\theta \text{ or } |\varphi-\phi| > \varepsilon_\phi, \quad (7)$$

where $\varepsilon_\theta$ and $\varepsilon_\phi$ are small numbers possibly depending on $\sigma_\theta$ and $\sigma_\phi$, respectively. Without loss of generality, we also assume that $\vartheta = \theta$ and $\varphi = \phi$ are the axes of symmetry of the function $\varrho(\vartheta, \varphi; \mu)$.

The relation (6) for a coherently distributed source provides the time invariance of the channel and some correlation for different angles at any time: specifically, the angular auto-correlation of the signal intensity (6) is

$$E\{\varsigma(\vartheta,\varphi,t)\varsigma^*(\vartheta',\varphi',t)\} = \zeta\varrho(\vartheta,\varphi;\mu)\varrho^*(\vartheta',\varphi';\mu), \quad (8)$$

where $*$ denotes the complex conjugate and $\zeta = E\{|s(t)|^2\}$. Eq. (8) implies that the signal components at different angles within a source are correlated mutually.

In terms of the steering vector, the coherently distributed source model (5) can be expressed as

$$\mathbf{x}(t) = s(t)\mathbf{b}(\mu) + \mathbf{n}(t), \quad (9)$$

where $\mathbf{b}(\mu)$ is the $L \times 1$ steering vector defined as

$$\mathbf{b}(\mu) = \int\int \mathbf{a}(\vartheta,\varphi)\varrho(\vartheta,\varphi;\mu)\,\mathrm{d}\vartheta\,\mathrm{d}\varphi. \quad (10)$$

As a common example of the coherently distributed source, assume that the deterministic angular weighting function $\varrho(\vartheta, \varphi; \mu)$ has the Gaussian shape

$$\varrho(\vartheta,\varphi;\mu) = \frac{1}{2\pi\sigma_\theta\sigma_\phi}\,\mathrm{e}^{-1/2((\vartheta-\theta)^2/\sigma_\theta^2+(\varphi-\phi)^2/\sigma_\phi^2)}. \quad (11)$$

Then, the closed form of the steering vector $\mathbf{b}(\mu)$ can be written as (see Appendix A)

$$
\begin{aligned}
[\mathbf{b}(\mu)]_k &= \int\int [\mathbf{a}(\vartheta,\varphi)]_k \varrho(\vartheta,\varphi;\mu)\,\mathrm{d}\vartheta\,\mathrm{d}\varphi \\
&\approx \mathrm{e}^{\mathrm{j}\eta\sin\theta\cos(\phi-\gamma_k)} \\
&\quad\times\int\int \mathrm{e}^{\mathrm{j}\eta(\tilde{\vartheta}\cos\theta\cos(\phi-\gamma_k)-\tilde{\varphi}\sin\theta\sin(\phi-\gamma_k))} \\
&\quad\times\varrho(\tilde{\vartheta}+\theta,\tilde{\varphi}+\phi;\mu)\,\mathrm{d}\tilde{\vartheta}\,\mathrm{d}\tilde{\varphi} \\
&= \mathrm{e}^{\mathrm{j}\eta\sin\theta\cos(\phi-\gamma_k)} g_k(\mu), \qquad (12)
\end{aligned}
$$

where $[\,\cdot\,]_k$ indicates the $k$th element of a vector and $g_k(\mu) = \mathrm{e}^{-0.5\eta^2(\sigma_\theta^2\cos^2\theta\cos^2(\phi-\gamma_k)+\sigma_\phi^2\sin^2\theta\sin^2(\phi-\gamma_k))}$ for small angular extensions $\sigma_\theta$ and $\sigma_\phi$. We would like to mention in passing that, when $\sigma_\theta$ and $\sigma_\phi$ are small, we can use (11) for $\vartheta-\theta\in[-\pi/2,\pi/2]$ and $\varphi-\phi\in[-\pi,\pi]$ although the Gaussian function is defined over $(-\infty,\infty)$.

Extending (9), the model when $q$ plane waves from $q$ sources with parameters $\mu_i=(\theta_i,\sigma_{\theta i},\phi_i,\sigma_{\phi i})$ $i=1,2,\ldots,q$, are incident on the UCA can be written as

$$
\begin{aligned}
\mathbf{x}(t) &= \sum_{i=1}^{q} s_i(t)\mathbf{b}_i + \mathbf{n}(t) \\
&= \mathbf{B}\mathbf{s}(t) + \mathbf{n}(t), \qquad (13)
\end{aligned}
$$

where $\mathbf{b}_i=\mathbf{b}(\mu_i)=\mathbf{b}(\theta_i,\sigma_{\theta_i},\phi_i,\sigma_{\phi_i})$, $\mathbf{B}=[\mathbf{b}_1,\mathbf{b}_2,\ldots,\mathbf{b}_q]$ is of size $L\times q$, and $\mathbf{s}(t)=[s_1(t),s_2(t),\ldots,s_q(t)]^{\mathrm{T}}$ is of size $q\times 1$.

## 3. Parameter estimation

In general, an optimum estimation method for point or distributed sources can provide an excellent performance at the cost of intensive computation. Since the computational complexity increases dramatically with high dimensional parameters, we have to sometimes find suboptimum methods to reduce the computational cost while sustaining the estimation performance within a tolerable level. It is noteworthy that a considerable simplification is possible by exploiting and utilizing the special array structure of the array geometry in the parameter estimation under distributed source models also, as it has been accomplished in the root-MUSIC and ESPRIT [9] for point sources.

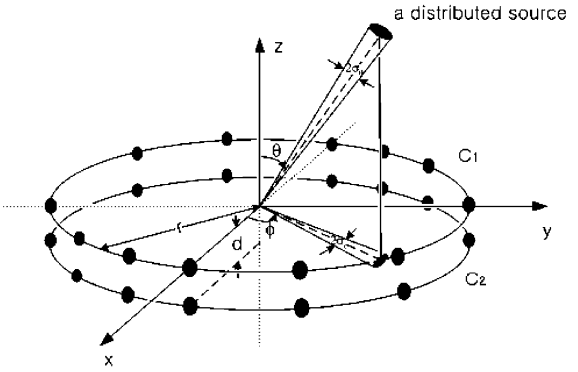


Fig. 1. Uniform circular array geometry.

In this section, we make use of a pair of UCAs, which will enable us to have a simplified DOA estimation method: we propose a sequential one-dimensional searching (SOS) method for estimating the nominal azimuth and elevation DOAs, based on the special array geometry of the UCA pair.

### 3.1. Array geometry, eigenstructure, and pre-processing

We assume that the antenna array is composed of two closely spaced identical uniform circular arrays $C_1$ and $C_2$. The two arrays are physically displaced from each other by a known distance $d$ vertically and the origin of the coordinate system is located at the center of $C_1$. Elements of $C_1$ and $C_2$ are displaced by an angle $\gamma_k=2\pi(k-1)/L$, for $k=1,2,\ldots,L$, from the $x$-axis. The position vectors are $\mathbf{p}_1=(r\cos\gamma_k,\ r\sin\gamma_k,0)$ and $\mathbf{p}_2=(r\cos\gamma_k,\ r\sin\gamma_k,-d)$ for $C_1$ and $C_2$, respectively. For reference, the array geometry is depicted in Fig. 1.

Consider a narrowband plane wave with wavenumber $k_0=2\pi/\lambda$ propagating in the direction $-\mathbf{r}$, where $\mathbf{r}=(\sin\theta\cos\phi,\sin\theta\sin\phi,\theta)$. The phase difference between the received signal at the origin and the received signal at element $k$ is $\psi_{k1}=\mathrm{e}^{\mathrm{j}k_0\mathbf{r}\cdot\mathbf{p}_1}=\mathrm{e}^{\mathrm{j}\eta\sin\theta\cos(\phi-\gamma_k)}$ and $\psi_{k2}=\mathrm{e}^{\mathrm{j}k_0\mathbf{r}\cdot\mathbf{p}_2}=\mathrm{e}^{\mathrm{j}\eta\sin\theta\cos(\phi-\gamma_k)}\mathrm{e}^{-\mathrm{j}k_0d\cos\theta}$ in $C_1$ and $C_2$, respectively.

The received signal vector in $C_1$ can be expressed as in (9), and that in $C_2$ is

$$\mathbf{y}(t) = s(t)\int\int \mathbf{a}(\vartheta,\varphi)\mathrm{e}^{-\mathrm{j}(2\pi d/\lambda)\cos\vartheta}\varrho(\vartheta,\varphi;\mu)\,\mathrm{d}\vartheta\,\mathrm{d}\varphi + \mathbf{v}(t) = s(t)\mathbf{c}(\mu) + \mathbf{v}(t), \tag{14}$$

where the $L \times 1$ steering vector $\mathbf{c}(\mu)$ is defined as

$$\mathbf{c}(\mu) = \int\int \mathbf{a}(\vartheta,\varphi)\mathrm{e}^{-\mathrm{j}(2\pi d/\lambda)\cos\vartheta}\varrho(\vartheta,\varphi;\mu)\,\mathrm{d}\vartheta\,\mathrm{d}\varphi \tag{15}$$

and $\mathbf{v}(t)$ is the $L \times 1$ noise vector with the same assumptions as those for the noise $\mathbf{n}(t)$ and is uncorrelated with both the signal and the noise $\mathbf{n}(t)$. It can be shown as in Appendix B that we have $\mathbf{c}(\mu) \approx \mathbf{b}(\mu)\,\mathrm{e}^{-\mathrm{j}(2\pi d/\lambda)\cos\theta}$ for small angular extensions, which in the matrix form can be extended to

$$\mathbf{C} \approx \mathbf{B}\Phi \tag{16}$$

for $q$ sources. In (16), $\mathbf{C} = [\mathbf{c}_1, \mathbf{c}_2, \ldots, \mathbf{c}_q]$ is of size $L \times q$, $\mathbf{c}_i = \mathbf{c}(\mu_i)$, and

$$\Phi = \mathrm{diag}(\mathrm{e}^{-\mathrm{j}(2\pi d/\lambda)\cos\theta_1}, \ldots, \mathrm{e}^{-\mathrm{j}(2\pi d/\lambda)\cos\theta_q}) \tag{17}$$

is of size $q \times q$. Note that both $\mathbf{b}(\mu)$ and $\mathbf{c}(\mu)$ depend on the angular weighting function but $\Phi$ does not. The total array output vector $\mathbf{z}(t) = \begin{bmatrix}\mathbf{x}(t)\\ \mathbf{y}(t)\end{bmatrix}$ of size $2L \times 1$ can be written as

$$\mathbf{z}(t) = \Upsilon\mathbf{s}(t) + \mathbf{u}(t), \tag{18}$$

where $\mathbf{u}(t) = \begin{bmatrix}\mathbf{n}(t)\\ \mathbf{v}(t)\end{bmatrix}$ and

$$\Upsilon = \begin{bmatrix}\mathbf{B}\\ \mathbf{B}\Phi\end{bmatrix} \tag{19}$$

is of size $2L \times q$.

Let $\mathbf{E}_s$ be the $2L \times q$ matrix whose columns are the eigenvectors corresponding to the $q$ largest eigenvalues of the $2L \times 2L$ covariance matrix $\mathbf{R}_z = E\{\mathbf{z}(t)\mathbf{z}^{\mathrm{H}}(t)\}$. Then, the subspace spanned by the columns of $\mathbf{E}_s$ is equal to the subspace spanned by the columns of the steering matrix $\Upsilon$, when the $q \times q$ signal (source) covariance matrix $\mathbf{P} = E\{\mathbf{s}(t)\mathbf{s}^{\mathrm{H}}(t)\}$ is of full rank. (Assuming that the distributed sources are uncorrelated mutually, we have $\mathbf{P} = \mathrm{diag}(\zeta_1, \zeta_2, \ldots, \zeta_q)$, $\zeta_i = E\{|s_i(t)|^2\}$.) Consequently, there exists a non-singular $q \times q$ matrix $\mathbf{W}$ such that $\mathbf{E}_s = \Upsilon\mathbf{W}$. In addition, the invariance structure (19) of the array allows the partition of $\mathbf{E}_s$ into two $L \times q$ matrices $\mathbf{E}_{s_1}$ and $\mathbf{E}_{s_2}$ composed of the first and last $L$ rows of $\mathbf{E}_s$, respectively, such that

$$\mathbf{E}_{s_1} = \mathbf{B}\mathbf{W} \tag{20}$$

and $\mathbf{E}_{s_2} = \mathbf{B}\Phi\mathbf{W}$. Note that the range spaces of $\mathbf{E}_{s_1}$ and $\mathbf{E}_{s_2}$ are the same and equal to the range space of $\mathbf{B}$: $R\{\mathbf{E}_{s_1}\} = R\{\mathbf{E}_{s_2}\} = R\{\mathbf{B}\}$, where $R\{\cdot\}$ denotes the range space of a matrix.

By employing ESPRIT methods, for example, in the DOA estimation, we can exploit the special array characteristic (the invariance structure) represented by (19). In this paper, we use the TLS-ESPRIT method [21] to obtain the initial inputs (estimates of the elevation DOAs $\theta_i$'s) to the SOS algorithm. Although the TLS-ESPRIT is applicable only to an array with a special geometry and experiences higher estimation errors than such other methods as the maximum likelihood (ML) and subspace fitting because it exploits only the translation between two identical arrays, it offers a high accuracy at a small computational cost and avoids some problems associated with the calibration for estimating the nominal elevation DOA.

From now on, we denote the $i$th nominal elevation DOA $\theta_i$ estimated by the TLS-ESPRIT as $\tilde{\theta}_i$, where

$$\tilde{\theta}_i = \cos^{-1}\left[-\lambda\frac{\arg(l_i)}{2\pi d}\right] \tag{21}$$

with $l_i$ the $i$th eigenvalue of a matrix used in the TLS-ESPRIT.

### 3.2. Sequential one-dimensional searching (SOS) method

Assume that we have a criterion function, which has the nominal azimuth and elevation DOAs as unknown parameters. When we estimate the two DOAs based on the criterion function, we have to generally solve a 2D optimization problem. Furthermore, the computational complexity grows rapidly as the number of sources increases. On the other hand, if we have some preliminary information on either the nominal azimuth or elevation DOA, it is anticipated that we can

estimate the other DOA by one-dimensional searching of the criterion function with much reduced complexity and computation.

We would thus like to propose a criterion function with which we can estimate the two nominal DOAs one by one with the help of preliminary estimates. Eventually, using the criterion function to be proposed, we first estimate the nominal azimuth DOA by the SOS method with the nominal elevation DOA estimate (21) obtained by the TLS-ESPRIT method. Then, we estimate the nominal elevation DOA with the nominal azimuth DOA estimated by the SOS procedure.

From (20), we have $\mathbf{B} = \mathbf{E}_{s_1}\mathbf{W}^{-1}$, or equivalently

$$\mathbf{b}_i = \mathbf{E}_{s_1}\mathbf{m}_i, \tag{22}$$

where the $i$th column vector $\mathbf{m}_i$ of $\mathbf{W}^{-1}$ is of size $q \times 1$. As shown in Appendix A, we also have

$$\mathbf{b}(\mu) \approx \Psi(\theta,\phi)\mathbf{b}^*(\mu) \tag{23}$$

and consequently

$$\mathbf{b}_i \approx \Psi_i \mathbf{b}_i^*, \tag{24}$$

where

$$\Psi(\theta,\phi) = \mathrm{diag}(\mathrm{e}^{\mathrm{j}2\eta\sin\theta\cos(\phi-\gamma_1)}, \mathrm{e}^{\mathrm{j}2\eta\sin\theta\cos(\phi-\gamma_2)}, \ldots, \mathrm{e}^{\mathrm{j}2\eta\sin\theta\cos(\phi-\gamma_L)}) \tag{25}$$

is an $L \times L$ diagonal matrix and $\Psi_i = \Psi(\theta_i,\phi_i)$.

Consider the $q \times q$ Hermitian matrix

$$\mathbf{T}(\theta,\phi) = \mathbf{E}_{s_1}^{\mathrm{H}}\Psi(\theta,\phi)\mathbf{E}_{s_1}^{*}\mathbf{E}_{s_1}^{\mathrm{T}}\Psi^*(\theta,\phi)\mathbf{E}_{s_1}, \tag{26}$$

which can easily be shown to be Gramian (in other words, positive definite or positive semi-definite) [6] since $\mathbf{T}(\theta,\phi) = \mathbf{D}^{\mathrm{H}}(\theta,\phi)\mathbf{D}(\theta,\phi)$ with the $q \times q$ matrix $\mathbf{D}(\theta,\phi) = \mathbf{E}_{s_1}^{\mathrm{T}}\Psi^*(\theta,\phi)\mathbf{E}_{s_1}$. (In passing, note that $\mathbf{D}^*(\theta,\phi) = \mathbf{D}^{\mathrm{H}}(\theta,\phi)$ and $\mathbf{D}^{\mathrm{T}}(\theta,\phi) = \mathbf{D}(\theta,\phi)$.) The eigenvalues of $\mathbf{T}(\theta,\phi)$ are positive numbers not larger than 1 as shown in Appendix C. In addition, denoting $\mathbf{T}_i = \mathbf{T}(\theta_i,\phi_i)$, we have

$$\begin{aligned}\mathbf{m}_i &= \mathbf{E}_{s_1}^{\mathrm{H}}\Psi_i\mathbf{E}_{s_1}^{*}\mathbf{m}_i^* \\ &= \mathbf{E}_{s_1}^{\mathrm{H}}\Psi_i\mathbf{E}_{s_1}^{*}\mathbf{E}_{s_1}^{\mathrm{T}}\Psi_i^*\mathbf{E}_{s_1}\mathbf{m}_i \\ &= \mathbf{T}_i\mathbf{m}_i\end{aligned} \tag{27}$$

from (22), (24), and $\mathbf{E}_{s_1}^{\mathrm{H}}\mathbf{E}_{s_1} = \mathbf{I}_q$. Eq. (27) tells us that $\mathbf{m}_i$ (which is the $i$th column vector of $\mathbf{W}^{-1}$) is an eigenvector of $\mathbf{T}_i$ and the corresponding eigenvalue is one, or equivalently, that the maximum value 1 of the eigenvalues of $\mathbf{T}(\theta,\phi)$ is attained at $(\theta,\phi) = (\theta_i,\phi_i)$. Therefore, when we are given $N$ measurements $\{\mathbf{z}(t),\ t = 1,2,\ldots,N\}$, one intuitively appealing and reasonable cost function based on these observations is

$$V(\theta,\phi) = \frac{1}{1-\hat{\lambda}_{\max}(\theta,\phi)} \tag{28}$$

and the estimates can be obtained from

$$(\hat{\theta},\hat{\phi}) = \arg\max_{\theta,\phi} V(\theta,\phi), \tag{29}$$

where $\hat{\lambda}_{\max}(\theta,\phi)$ denotes the maximum eigenvalue of an estimate $\hat{\mathbf{T}}(\theta,\phi)$ of $\mathbf{T}(\theta,\phi)$. (In other words, $\hat{\lambda}_{\max}(\theta,\phi)$ is the $q$th order statistic [23] $\hat{\lambda}_{[q]}(\theta,\phi)$ among the $q$ eigenvalues $\{\hat{\lambda}_1(\theta,\phi), \hat{\lambda}_2(\theta,\phi),\ldots,\hat{\lambda}_q(\theta,\phi)\}$ of $\hat{\mathbf{T}}(\theta,\phi)$ at any given $(\theta,\phi)$.) Here, $\hat{\mathbf{T}}(\theta,\phi) = \hat{\mathbf{E}}_{s_1}^{\mathrm{H}}\Psi(\theta,\phi)\hat{\mathbf{E}}_{s_1}^{*}\hat{\mathbf{E}}_{s_1}^{\mathrm{T}}\Psi^*(\theta,\phi)\hat{\mathbf{E}}_{s_1}$ is determined by $\Psi(\theta,\phi)$ and the first $L$ rows $\hat{\mathbf{E}}_{s_1}$ of the sample signal eigenvector matrix $\hat{\mathbf{E}}_s$ obtained from the sample covariance matrix $\hat{\mathbf{R}}_z = 1/N\ \sum_{t=1}^{N}\mathbf{z}(t)\mathbf{z}^{\mathrm{H}}(t)$.

Let $\hat{\mathbf{b}} = \hat{\mathbf{E}}_{s_1}\hat{\mathbf{m}}$ with $\hat{\mathbf{m}}$ the $q \times 1$ eigenvector corresponding to $\hat{\lambda}_{\max}(\theta,\phi)$ and $\hat{\mathbf{E}}_{n_1}$ the first $L$ rows of the sample noise eigenvector matrix $\hat{\mathbf{E}}_n$ obtained from $\hat{\mathbf{R}}_z$. Then, using $\hat{\mathbf{E}}_{s_1}\hat{\mathbf{E}}_{s_1}^{\mathrm{H}} + \hat{\mathbf{E}}_{n_1}\hat{\mathbf{E}}_{n_1}^{\mathrm{H}} = \mathbf{I}_L$, $\Psi(\theta,\phi)\Psi^*(\theta,\phi) = \mathbf{I}_L$, $\hat{\mathbf{E}}_{s_1}^{\mathrm{H}}\hat{\mathbf{E}}_{s_1} = \mathbf{I}_q$, $\hat{\mathbf{m}}^{\mathrm{H}}\hat{\mathbf{m}} = 1$, and $\hat{\mathbf{b}} \approx \Psi(\theta,\phi)\hat{\mathbf{b}}^*$ inferred from (23) analogically, we have

$$\begin{aligned}1-\hat{\lambda}_{\max}(\theta,\phi) &= 1-\hat{\mathbf{m}}^{\mathrm{H}}\hat{\mathbf{T}}(\theta,\phi)\hat{\mathbf{m}} \\ &\approx \hat{\mathbf{b}}^{\mathrm{T}}\hat{\mathbf{E}}_{n_1}^{*}\hat{\mathbf{E}}_{n_1}^{\mathrm{T}}\hat{\mathbf{b}}^*\end{aligned} \tag{30}$$

after some steps similar to those in Appendix C. It is noteworthy that the right-hand side of (30) is basically the same in functional form as the pseudo-spectrum of the DSPE algorithm [25] and the MUSIC null-spectrum [16]. We can show that this term should theoretically vanish at $(\theta,\phi) = (\theta_i,\phi_i)$, $i = 1,2,\ldots,q$ due to the orthogonality property between the steering vector and noise eigenvector matrix. Specifically, we have $\hat{\mathbf{b}}^{\mathrm{T}}\hat{\mathbf{E}}_{n_1}^{*}\hat{\mathbf{E}}_{n_1}^{\mathrm{T}}\hat{\mathbf{b}}^* \to \mathbf{b}^{\mathrm{T}}\mathbf{E}_{n_1}^{*}\mathbf{E}_{n_1}^{\mathrm{T}}\mathbf{b}^*$ assuming that $\hat{\mathbf{b}} \to \mathbf{E}_{s_1}\mathbf{m}$ and $\hat{\mathbf{E}}_{n_1} \to \mathbf{E}_{n_1}$ as $N \to \infty$, where $\mathbf{m}$ is the eigenvector corresponding to the largest eigenvalue of $\mathbf{T}(\theta,\phi)$ and $\mathbf{E}_{n_1}$ is the first $L$ rows of the noise eigenvector matrix $\mathbf{E}_n$ obtained

from the covariance matrix $\mathbf{R}_z$. Consequently,

$$1-\hat{\lambda}_{\max}(\theta_i,\phi_i)\to \mathbf{b}_i^{\mathrm{T}}\mathbf{E}_{n_1}^{*}\mathbf{E}_{n_1}^{\mathrm{T}}\mathbf{b}_i^{*} = \|\mathbf{b}_i^{\mathrm{H}}\mathbf{E}_{n_1}\|^2 = 0 \quad (31)$$

as $N\to\infty$ since $\mathbf{E}_{s_1}\mathbf{m}|_{(\theta,\phi)=(\theta_i,\phi_i)}=\mathbf{b}_i$ and the steering vector $\mathbf{b}$ and noise eigenvector matrix $\mathbf{E}_{n_1}$ are orthogonal when $(\theta,\phi)=(\theta_i,\phi_i)$, or since $(\mathbf{E}_{s_1}\mathbf{m}_i)^{\mathrm{H}}\mathbf{E}_{n_1}=\mathbf{b}_i^{\mathrm{H}}\mathbf{E}_{n_1}=\mathbf{0}$.

Employing preliminary estimates either of the nominal elevation DOAs or of nominal azimuth DOAs, the estimation method based on the cost function (28) and estimation procedure (29) can be simplified to a one-dimensional searching method. Specifically, we first use in (29) the preliminary estimates (21) obtained from the TLS-ESPRIT to estimate the nominal azimuth DOA $\phi_i$. With the estimated nominal azimuth DOA in turn, we use (29) again to more accurately estimate the nominal elevation DOA $\theta_i$. This proposed method based on the cost function (28) and the preliminary estimates (21) will be called the SOS method.

We summarize the proposed SOS algorithm:

1. Compute the sample covariance matrix $\hat{\mathbf{R}}_z=1/N\sum_{t=1}^{N}\mathbf{z}(t)\mathbf{z}^{\mathrm{H}}(t)$ using the measurements $\{\mathbf{z}(t),\ t=1,2,\ldots,N\}$ obtained from $C_1$ and $C_2$.
2. Through the eigen-decomposition of $\hat{\mathbf{R}}_z$, obtain the sample signal eigenvector matrix $\hat{\mathbf{E}}_s$, and subsequently, $\hat{\mathbf{E}}_{s_1}$ and $\hat{\mathbf{T}}(\theta,\phi)$.
3. Obtain the nominal elevation estimates $\tilde{\theta}_i$, $i=1,2,\ldots,q$ by the TLS-ESPRIT algorithm from (21).
4. Estimate the nominal azimuth DOA $\phi_i$ using $\theta_i=\tilde{\theta}_i$ obtained at Step 3:
$$\hat{\phi}_i=\arg\max_{\phi} V(\tilde{\theta}_i,\phi). \quad (32)$$
5. Estimate the nominal elevation DOA $\theta_i$ using $\phi_i=\hat{\phi}_i$ obtained at Step 4:
$$\hat{\theta}_i=\arg\max_{\theta} V(\theta,\hat{\phi}_i). \quad (33)$$
6. Repeat Steps 4 and 5 for $i=1,2,\ldots,q$.

Although we have not specifically investigated here, we can anticipate almost the same estimation results from the SOS method when we estimate the nominal azimuth DOA first as the preliminary estimates and when we use other methods than the TLS-ESPRIT in the preliminary stage (except that the computational complexity in the preliminary stage might depend on the specific method.) In addition, from (16) to (21) and (25) to (28), it is clear that the proposed SOS algorithm does not depend practically on the specific angular weighting functions of distributed sources when the angular extensions $\sigma_\theta$ and $\sigma_\phi$ are small. This means that the proposed SOS algorithm can be applied to also a scenario in which distributed sources may have different angular weighting functions.

The SOS method is a suboptimum spectral-based method (as is the DSPE) and is applicable when there exists a special array geometry, while the ML and weighted subspace fitting (WSF) can be used with arbitrary array geometry and generally provide (almost) optimum performance at the expense of higher computational complexity: there is always a tradeoff between the performance and computational complexity.

## 4. Simulation results

In this section, we investigate the performance of the proposed SOS algorithm through some simulation experiments. Assume that each of $C_1$ and $C_2$ has $L=10$ sensors, the distance between the two arrays is $d=0.1\lambda$, and the spacing between adjacent sensors is $0.5\lambda$. The signal-to-noise ratio (SNR) is defined as $-10\log\sigma^2$.

In the first example, we numerically illustrate the proposed SOS algorithm for two equipower uncorrelated narrowband coherently distributed sources with SNR = 15 dB. The two distributed sources have Gaussian shaped angular weighting functions both in azimuth and elevation with parameters $\mu_1=(60^\circ,2^\circ,10^\circ,3^\circ)$ and $\mu_2=(75^\circ,1.5^\circ,65^\circ,4^\circ)$. The preliminary estimates of the nominal elevation DOAs by the TLS-ESPRIT are $\tilde{\theta}_1=59.43^\circ$ and $\tilde{\theta}_2=74.65^\circ$. Fig. 2 shows the one-dimensional spectra for the estimation of the nominal azimuth DOA $\phi_1$ with the cost function (28) and conventional MUSIC with $\theta_1=\tilde{\theta}_1$. Fig. 3 shows the one-dimensional spectra for the estimation of the nominal elevation DOA $\theta_1$ with the cost function (28) and conventional MUSIC with $\phi_1=\hat{\phi}_1$: clearly, both methods have

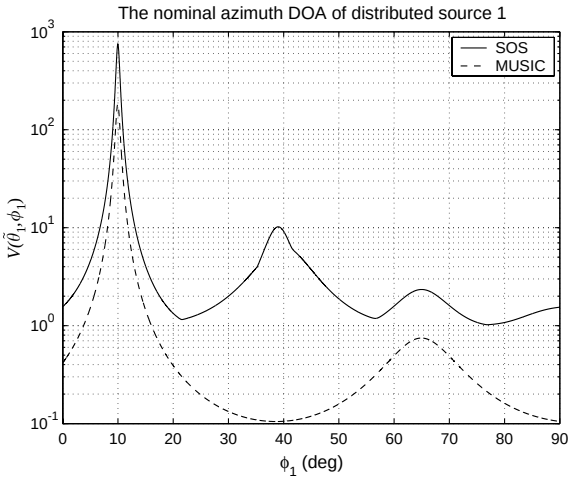


Fig. 2. One-dimensional searching spectrum for the nominal azimuth $\phi_1$ of the first distributed source with the preliminary estimate $\tilde{\theta}_1 = 59.43°$ from the TLS-ESPRIT: $\hat{\phi}_1 = 9.98°$ (SOS) and $\hat{\phi}_1 = 9.96°$ (MUSIC).

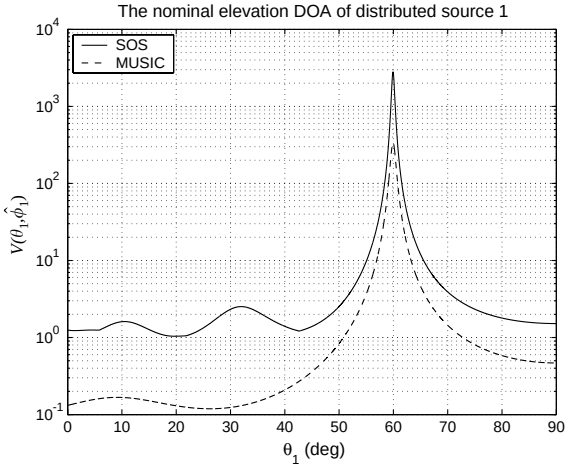


Fig. 3. One-dimensional searching spectrum for the nominal elevation $\theta_1$ of the first distributed source with $\hat{\phi}_1 = 9.98°$ (SOS) and $\hat{\phi}_1 = 9.96°$ (MUSIC) estimated in Fig. 2: $\hat{\theta}_1 = 59.93°$ (SOS) and $\hat{\theta}_1 = 59.89°$ (MUSIC).

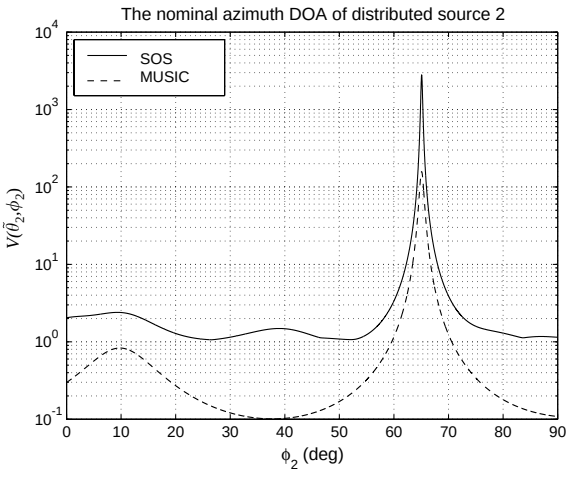


Fig. 4. One-dimensional searching spectrum for the nominal azimuth $\phi_2$ of the second distributed source with the preliminary estimate $\tilde{\theta}_2 = 74.65°$ from the TLS-ESPRIT: $\hat{\phi}_2 = 65.07°$ (SOS) and $\hat{\phi}_2 = 65.15°$ (MUSIC).

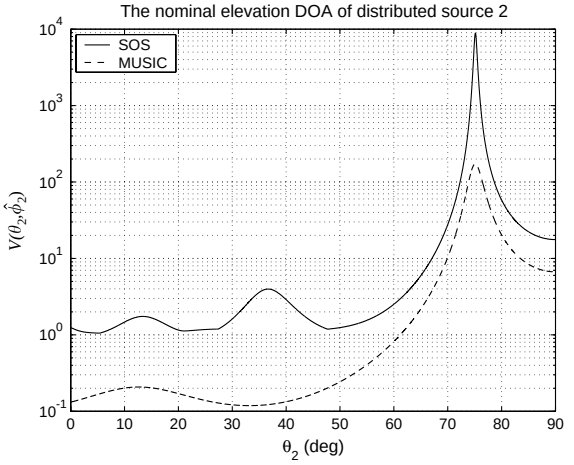


Fig. 5. One-dimensional searching spectrum for the nominal elevation $\theta_2$ of the second distributed source with $\hat{\phi}_2 = 65.07°$ (SOS) and $\hat{\phi}_2 = 65.15°$ (MUSIC) estimated from Fig. 4: $\hat{\theta}_2 = 75.11°$ (SOS) and $\hat{\theta}_2 = 75.15°$ (MUSIC).

peaks close to $\phi_1 = 10°$ and $\theta_1 = 60°$ for the first source. Similarly, the results for the second distributed source are illustrated in Figs. 4 and 5. The values of the spectrum of the MUSIC is generally lower than those of the SOS in the figures: note that what is important is the 'relative height', not the 'absolute value' of the peak. The MUSIC method as well as the SOS exhibits the peaks at the true DOA. We have also obtained the variances of the estimation errors for both methods as shown in Table 1. The table shows that the SOS method provides a gain of roughly 5% for the estimation of 2D DOAs in comparison with the MUSIC for small angular extensions.

Table 1
Variances of the 2D DOA estimation errors for the SOS algorithm and conventional MUSIC obtained from simulations with 100 trials ($N = 100$)

| Method | Distributed source 1 | | Distributed source 2 | |
|---|---|---|---|---|
| | $\mathrm{var}(\phi_1 - \hat{\phi}_1)$ | $\mathrm{var}(\theta_1 - \hat{\theta}_1)$ | $\mathrm{var}(\phi_2 - \hat{\phi}_2)$ | $\mathrm{var}(\theta_2 - \hat{\theta}_2)$ |
| SOS | 0.0715 | 0.1276 | 0.0789 | 0.2378 |
| Conventional MUSIC | 0.0743 | 0.1342 | 0.0823 | 0.2649 |

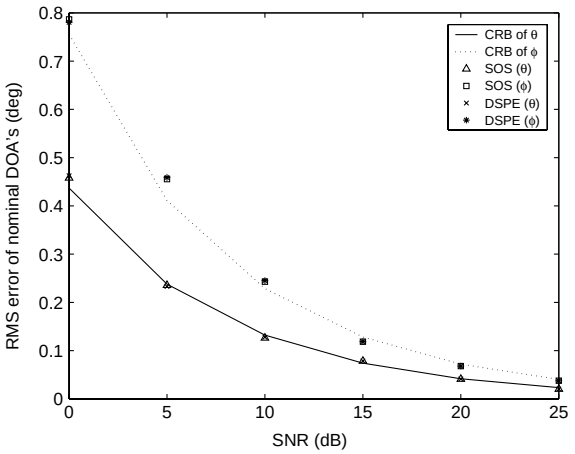


Fig. 6. Estimation performance of the SOS and DSPE algorithms: the RMS error of the nominal DOAs versus SNR for a distributed source with $(\theta, \sigma_\theta, \phi, \sigma_\phi) = (30°, 2°, 10°, 5°)$.

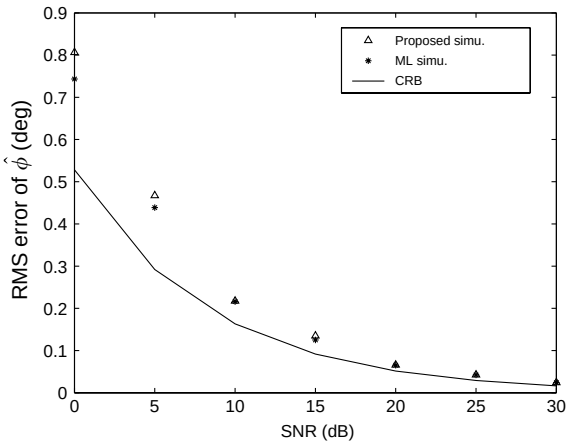


Fig. 7. The RMS error of $\hat{\phi}$ versus SNR for a distributed source with $(\theta, \sigma_\theta, \phi, \sigma_\phi) = (30°, 2°, 10°, 5°)$.

In the second example, we compare the SOS method when (29) is used directly without preliminary estimates (2D search) with the DSPE algorithm (four-dimensional search) for a Gaussian-shaped distributed source at $\mu = (30°, 2°, 10°, 5°)$ with a single UCA of $L = 10$ sensors: the comparison is performed based only on the cost functions of the two methods. Fig. 6 shows that the SOS method provides almost the same performance as the DSPE and is statistically efficient.

In the third example, we examine the estimation performance of the proposed SOS algorithm in comparison with the ML method for a Gaussian-shaped distributed source with $\mu = (30°, 2°, 10°, 5°)$. We have used a quasi-Newton algorithm to estimate the parameters in the ML method. A Monte Carlo simulation of 200 independent runs with $N = 100$ snapshots for each trial has been performed. The root-mean-square (RMS) error values of the nominal azimuth $\hat{\phi}$ and nominal elevation $\hat{\theta}$ estimated by the SOS and ML methods as well as the Cramer-Rao lower bound (CRB) are illustrated at different SNR in Figs. 7 and 8. We can clearly observe that the DOA estimates not only of the ML method but also of the SOS method attain the CRB as the SNR increases.

Figs. 9 and 10 show the RMS errors of the nominal azimuth $\hat{\phi}$ and elevation $\hat{\theta}$ when $\theta = 30°$, $\sigma_\theta = 2°$, $\phi = 10°$, the angular extension $\sigma_\phi$ varies, and SNR $=$ 15 dB: it is observed that the variation of the RMS errors in the SOS and ML methods are rather small even when the angular extension $\sigma_\phi$ increases. This is partly because of the characteristics of the UCA steering vector for a coherently distributed source.

Figs. 11 and 12 show the weighting values (defined as (A.5)) of the $k$th elements for the UCA and ULA steering vectors for a Gaussian and a Laplacian-shaped distributed sources, respectively, when the angular

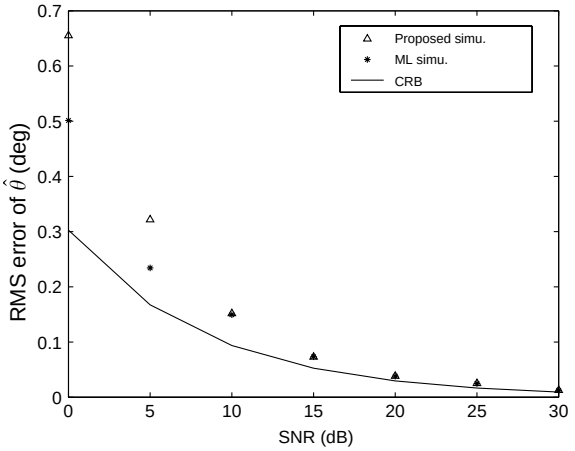


Fig. 8. The RMS error of $\hat{\theta}$ versus SNR for a distributed source with $(\theta, \sigma_\theta, \phi, \sigma_\phi) = (30°, 2°, 10°, 5°)$.

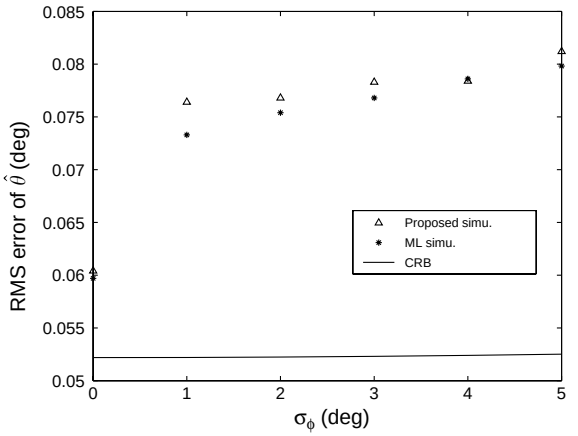


Fig. 10. The RMS error of $\hat{\theta}$ versus the angular extension $\sigma_\phi$ for a distributed source with $(\theta, \sigma_\theta, \phi) = (30°, 2°, 10°)$ when SNR = 15 dB.

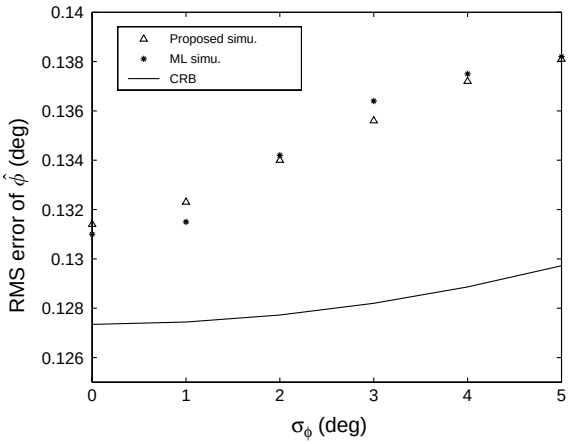


Fig. 9. The RMS error of $\hat{\phi}$ versus the angular extension $\sigma_\phi$ for a distributed source with $(\theta, \sigma_\theta, \phi) = (30°, 2°, 10°)$ when SNR = 15 dB.

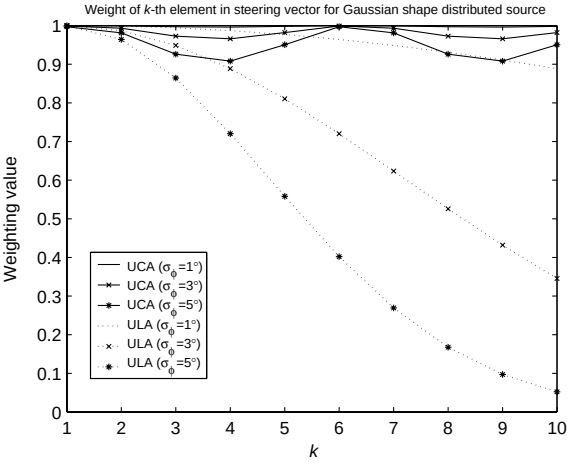


Fig. 11. The weighting values of the $k$th elements for the steering vectors of the UCA and ULA for a Gaussian shaped distributed source: $\phi = 10°$, $L = 10$, $\sigma_\phi = 1°$ (no marker), 3° (x), and 5° (*).

extension $\sigma_\phi$ has three different values, the nominal azimuth DOA is $\phi = 10°$, and the number of sensors is $L = 10$. Note that the weighting values are all 1 for a point source. For simplicity, we consider only azimuth DOA. It is conceivable that the weighting values for the UCA steering vector undergo less variation as the angular extensions increase: this means that the UCA is robust against the change of the angular extensions, as shown to a certain degree in [10] also.

Clearly, the proposed SOS algorithm provides a sufficiently good estimation accuracy as well as computational simplicity (compared to direct 2D methods) for estimating the nominal azimuth and elevation DOAs. Note that the computational requirement of the SOS method is in general $2q$ one-dimensional searches, that of the DSPE is $q$ four-dimensional searches, and that of the ML method is a $4q$-dimensional search for $q$ distributed sources, although the DSPE and ML

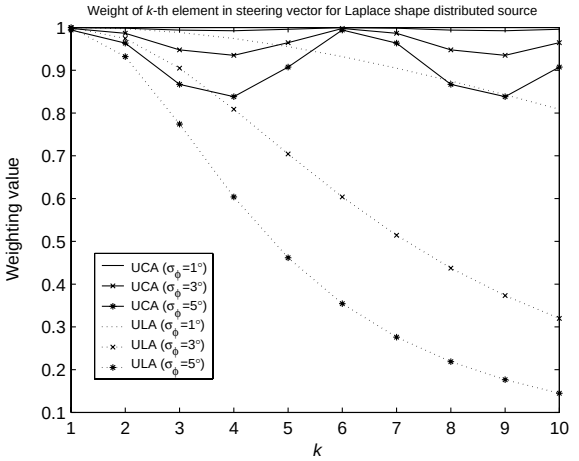


Fig. 12. The weighting values of the $k$th elements for the steering vectors of the UCA and ULA for a Laplacian shaped distributed source: $\phi = 10°$, $L = 10$, $\sigma_\phi = 1°$ (no marker), 3° (x), and 5° (*).

would estimate the angular extensions also, where $p$-dimensional search means a full $p$-dimensional numerical optimization.

## 5. Concluding remark

In this paper, we have considered the modeling of coherently distributed sources and the estimation of the two-dimensional DOAs of distributed sources with a pair of uniform circular arrays. We have proposed a low-complexity algorithm estimating the nominal azimuth and elevation DOAs one by one with only one-dimensional searches based on the eigenstructure between the steering matrix and the signal subspace of distributed sources.

The proposed SOS algorithm requires a pre-processing stage at which preliminary estimates of the nominal elevation DOAs are obtained: in this paper, we have employed the ESPRIT algorithm for the pre-processing, making use of the special geometry of a pair of uniform circular arrays. The proposed SOS algorithm provides as good an estimation performance as that of the maximum likelihood method at high SNR while requiring only one-dimensional searches. The proposed SOS method has been shown to be useful also in situations where there exist a number of distributed sources having different angular weighting functions. The proposed SOS method would be useful, for example, as the pre-processor of a beamforming method based on the nominal DOAs of distributed sources and also for the localization of distributed sources in three-dimensional practical environment.

## Acknowledgements

This research was supported by an internal grant of Queen's University and by Korea Science and Engineering Foundation (KOSEF) under Grant R01-2000-000-00259-0, for which the authors would like to express their thanks. The authors also wish to thank the anonymous reviewers for their helpful and constructive comments and suggestions.

## Appendix A. Approximation to the steering vector for small angular extensions

We have

$$[\mathbf{b}(\mu)]_k = \int\int [\mathbf{a}(\vartheta,\varphi)]_k \varrho(\vartheta,\varphi;\mu)\,\mathrm{d}\vartheta\,\mathrm{d}\varphi$$
$$= \int\int \mathrm{e}^{\mathrm{j}\eta\sin(\theta+\tilde{\vartheta})\cos(\phi+\tilde{\varphi}-\gamma_k)} \times \varrho(\tilde{\vartheta}+\theta,\tilde{\varphi}+\phi;\mu)\,\mathrm{d}\tilde{\vartheta}\,\mathrm{d}\tilde{\varphi} \quad (A.1)$$

with the change of variables $\vartheta - \theta = \tilde{\vartheta}$ and $\varphi - \phi = \tilde{\varphi}$. Due to (7), the computation result of (A.1) amounts to that of (A.1) for only small $\tilde{\vartheta}$ and $\tilde{\varphi}$.

Now, for small values of $\tilde{\vartheta}$ and $\tilde{\varphi}$, the functions $\sin\tilde{\vartheta}$, $\cos\tilde{\vartheta}$, $\sin\tilde{\varphi}$, and $\cos\tilde{\varphi}$ can be approximated by the first terms in the Taylor series expansions. Using the trigonometric identity $\sin(\alpha+\beta) = \sin\alpha\cos\beta + \cos\alpha\sin\beta$ and $\cos(\alpha+\beta) = \cos\alpha\cos\beta - \sin\alpha\sin\beta$, we obtain

$$\mathrm{e}^{\mathrm{j}\eta\sin(\theta+\tilde{\vartheta})\cos(\phi+\tilde{\varphi}-\gamma_k)}$$
$$\approx \mathrm{e}^{\mathrm{j}\eta(\sin\theta+\tilde{\vartheta}\cos\theta)(\cos(\phi-\gamma_k)-\tilde{\varphi}\sin(\phi-\gamma_k))}$$
$$\simeq \mathrm{e}^{\mathrm{j}\eta\sin\theta\cos(\phi-\gamma_k)} \times \mathrm{e}^{\mathrm{j}\eta(\tilde{\vartheta}\cos\theta\cos(\phi-\gamma_k)-\tilde{\varphi}\sin\theta\sin(\phi-\gamma_k))}, \quad (A.2)$$

where we assume that $\tilde{\vartheta}\tilde{\varphi} \approx 0$ and consequently $e^{-j\eta\tilde{\vartheta}\tilde{\varphi}\cos\theta\sin(\phi-\gamma_k)} \simeq 1$. Using (A.2), we can rewrite (A.1) as

$$[\mathbf{b}(\mu)]_k \approx e^{j\eta\sin\theta\cos(\phi-\gamma_k)} g_k(\mu) \tag{A.3}$$

or

$$\mathbf{b}(\mu) \approx \mathbf{a}(\theta,\phi) \odot \mathbf{g}(\mu) \tag{A.4}$$

in vector notation, where

$$g_k(\mu) = \int\int e^{j\eta(\tilde{\vartheta}\cos\theta\cos(\phi-\gamma_k) - \tilde{\varphi}\sin\theta\sin(\phi-\gamma_k))} \times \varrho(\tilde{\vartheta}+\theta, \tilde{\varphi}+\phi;\mu)\,d\tilde{\vartheta}\,d\tilde{\varphi}, \tag{A.5}$$

$\odot$ is the element-by-element product, and $\mathbf{g}(\mu) = [g_k(\mu)]$ is an $L\times 1$ real-valued vector depending on the angular weighting function $\varrho(\vartheta,\varphi;\mu)$. Clearly, $g_k(\mu)$ is a real-valued function since $\varrho(\tilde{\vartheta}+\theta,\tilde{\varphi}+\phi;\mu)$ is an even function of $\tilde{\vartheta}$ and $\tilde{\varphi}$ because of the symmetry assumption given in Section 2. Note that we get

$$\mathbf{b}(\mu) \approx \Psi(\theta,\phi)\mathbf{b}^*(\mu) \tag{A.6}$$

from (A.4) and $\mathbf{b}^*(\mu) \approx \mathbf{a}^*(\theta,\phi) \odot \mathbf{g}(\mu)$ for small angular extensions $\sigma_\theta$ and $\sigma_\phi$.

Let us consider two examples of the approximate closed form (A.4) of $\mathbf{b}(\mu)$. Assume the Gaussian shaped angular weighting function (11). Using the integral formula [11] $\int_{-\infty}^{\infty} e^{-q^2x^2} e^{jp(x+\lambda)}\,dx = \sqrt{\pi}e^{-(p^2/4q^2)}e^{jp\lambda}/q$, the right-hand side of (A.5) can be written as

$$\frac{1}{2\pi\sigma_\theta\sigma_\phi}\int e^{j\tilde{\vartheta}\eta\cos\theta\cos(\phi-\gamma_k)} e^{-(\tilde{\vartheta}^2/2\sigma_\theta^2)}\,d\tilde{\vartheta} \times \int e^{-j\tilde{\varphi}\eta\sin\theta\sin(\phi-\gamma_k)} e^{-(\tilde{\varphi}^2/2\sigma_\phi^2)}\,d\tilde{\varphi}, \tag{A.7}$$

which in turn results in

$$g_k(\mu) = e^{-\sigma_\theta^2/2(\eta\cos\theta\cos(\phi-\gamma_k))^2} \times e^{-\sigma_\phi^2/2(\eta\sin\theta\sin(\phi-\gamma_k))^2}. \tag{A.8}$$

Thus, the approximate closed form of the steering vector $\mathbf{b}(\mu)$ is

$$[\mathbf{b}(\mu)]_k \approx [\mathbf{a}(\theta,\phi)]_k \times e^{-0.5\eta^2(\sigma_\theta^2\cos^2\theta\cos^2(\phi-\gamma_k)+\sigma_\phi^2\sin^2\theta\sin^2(\phi-\gamma_k))}. \tag{A.9}$$

Similarly, when the angular weighting function is Laplacian shaped

$$\varrho(\tilde{\vartheta},\tilde{\varphi};\mu) = \frac{1}{2\sigma_\theta\sigma_\phi} e^{-(\sqrt{2}|\tilde{\vartheta}-\theta|/\sigma_\theta + \sqrt{2}|\tilde{\varphi}-\phi|/\sigma_\phi)}, \tag{A.10}$$

we have

$$\begin{aligned}[\mathbf{b}(\mu)]_k &\approx [\mathbf{a}(\theta,\phi)]_k \times \left(\frac{1}{\sqrt{2}\sigma_\theta}\int e^{j\tilde{\vartheta}\eta\cos\theta\cos(\phi-\gamma_k)} e^{-(\sqrt{2}|\tilde{\vartheta}|/\sigma_\theta)}\,d\tilde{\vartheta}\right) \times \left(\frac{1}{\sqrt{2}\sigma_\phi}\int e^{-j\tilde{\varphi}\eta\sin\theta\sin(\phi-\gamma_k)} e^{-(\sqrt{2}|\tilde{\varphi}|/\sigma_\phi)}\,d\tilde{\varphi}\right) \\ &= [\mathbf{a}(\theta,\phi)]_k \left(\frac{1}{1+(\eta\sigma_\theta\cos\theta\cos(\phi-\gamma_k))^2}\right) \times \left(\frac{1}{1+(\eta\sigma_\phi\sin\theta\sin(\phi-\gamma_k))^2}\right)\end{aligned} \tag{A.11}$$

using [11] $\int_0^\infty e^{-px}\sin(vx+\varepsilon)\,dx = (v\cos\varepsilon + p\sin\varepsilon)/(p^2+v^2)$, $p>0$, and $\int_0^\infty e^{-px}\cos(vx+\varepsilon)\,dx = (p\cos\varepsilon - v\sin\varepsilon)/(p^2+v^2)$, $p>0$.

## Appendix B. Relationship between the steering vectors of $C_1$ and $C_2$

The steering vector of $C_2$ is obtained from

$$\begin{aligned}[\mathbf{c}(\mu)]_k &= \iint [\mathbf{a}(\vartheta,\varphi)]_k e^{-j(2\pi d/\lambda)\cos\vartheta}\varrho(\vartheta,\varphi;\mu)\,d\vartheta\,d\varphi \\ &= \int\int e^{j\eta\sin(\theta+\tilde{\vartheta})\cos(\phi+\tilde{\varphi}-\gamma_k)} e^{-j(2\pi d/\lambda)\cos(\theta+\tilde{\vartheta})} \times \varrho(\tilde{\vartheta}+\theta,\tilde{\varphi}+\phi;\mu)\,d\tilde{\vartheta}\,d\tilde{\varphi}\end{aligned} \tag{B.1}$$

with the change of variables $\vartheta-\theta=\tilde{\vartheta}$ and $\varphi-\phi=\tilde{\varphi}$. Following the steps similar to those we have done in (A.2) for small angular extensions $\sigma_\theta$ and $\sigma_\phi$, the

right-hand side of (B.1) can be written as

$$\int\int e^{j\eta(\sin\theta+\tilde{\vartheta}\cos\theta)(\cos(\phi-\gamma_k)-\tilde{\varphi}\sin(\phi-\gamma_k))} \times e^{-j(2\pi d/\lambda)(\cos\theta-\tilde{\vartheta}\sin\theta)} \times \varrho(\tilde{\vartheta}+\theta,\tilde{\varphi}+\phi;\mu)\,d\tilde{\vartheta}\,d\tilde{\varphi}. \quad (B.2)$$

Assuming $2\pi d\tilde{\vartheta}/\lambda \simeq 0$ when $d/\lambda \ll 1$ and $\tilde{\vartheta} \approx 0$, we have $e^{-j(2\pi d/\lambda)(\cos\theta-\tilde{\vartheta}\sin\theta)} \approx e^{-j(2\pi d/\lambda)\cos\theta}$. Thus, the approximate closed form of the steering vector $\mathbf{c}(\mu)$ is obtained from

$$[\mathbf{c}(\mu)]_k \approx e^{-j(2\pi d/\lambda)\cos\theta} e^{j\eta\sin\theta\cos(\phi-\gamma_k)} g_k(\mu). \quad (B.3)$$

From (A.3) and (B.3), we have

$$\mathbf{c}(\mu) \approx e^{-j(2\pi d/\lambda)\cos\theta}\mathbf{b}(\mu) \quad (B.4)$$

for small angular extensions $\sigma_\theta$ and $\sigma_\phi$.

## Appendix C. Characteristics of the eigenvalues of $\mathbf{T}(\theta,\phi)$

Using the definition (26) of $\mathbf{T}(\theta,\phi)$, the eigenvalue $\lambda_k(\theta,\phi)$ corresponding to a $q\times 1$ unit-norm eigenvector $\mathbf{g}_k(\theta,\phi)$, $k=1,2,\ldots,q$, of $\mathbf{T}(\theta,\phi)$ can be written in a singular Hermitian form of rank $q$ as

$$\begin{aligned}\lambda_k(\theta,\phi) &= \mathbf{g}_k^H(\theta,\phi)\mathbf{T}(\theta,\phi)\mathbf{g}_k(\theta,\phi)\\ &= \mathbf{g}_k^H(\theta,\phi)\mathbf{E}_{s_1}^H\Psi(\theta,\phi)\mathbf{E}_{s_1}^*\mathbf{E}_{s_1}^T \times \Psi^*(\theta,\phi)\mathbf{E}_{s_1}\mathbf{g}_k(\theta,\phi)\\ &= \mathbf{p}_k^H(\theta,\phi)\mathbf{E}_{s_1}^*\mathbf{E}_{s_1}^T\mathbf{p}_k(\theta,\phi) \quad (C.1)\end{aligned}$$

from $\mathbf{T}(\theta,\phi)\mathbf{g}_k(\theta,\phi) = \lambda_k(\theta,\phi)\mathbf{g}_k(\theta,\phi)$, where $\mathbf{p}_k(\theta,\phi) = \Psi^*(\theta,\phi)\mathbf{E}_{s_1}\mathbf{g}_k(\theta,\phi)$ is of size $L\times 1$: note that we have $\mathbf{p}_k^H(\theta,\phi)\mathbf{p}_k(\theta,\phi) = \mathbf{g}_k^H(\theta,\phi)\mathbf{E}_{s_1}^H\Psi(\theta,\phi)\Psi^*(\theta,\phi)\mathbf{E}_{s_1}\mathbf{g}_k(\theta,\phi) = \mathbf{g}_k^H(\theta,\phi)\mathbf{E}_{s_1}^H\mathbf{E}_{s_1}\mathbf{g}_k(\theta,\phi) = 1$ since $\Psi(\theta,\phi)\Psi^*(\theta,\phi) = \mathbf{I}_L$, $\mathbf{E}_{s_1}^H\mathbf{E}_{s_1} = \mathbf{I}_q$, and $\mathbf{g}_k^H(\theta,\phi)\mathbf{g}_k(\theta,\phi) = 1$. From the orthonormality $\mathbf{E}_{s_1}\mathbf{E}_{s_1}^H + \mathbf{E}_{n_1}\mathbf{E}_{n_1}^H = \mathbf{I}_L$ of the signal and noise eigenvectors, we have $\mathbf{E}_{s_1}^*\mathbf{E}_{s_1}^T = \mathbf{I}_L - \mathbf{E}_{n_1}^*\mathbf{E}_{n_1}^T$. Then, (C.1) can be rewritten as

$$\begin{aligned}\lambda_k(\theta,\phi) &= \mathbf{p}_k^H(\theta,\phi)(\mathbf{I}_L - \mathbf{E}_{n_1}^*\mathbf{E}_{n_1}^T)\mathbf{p}_k(\theta,\phi)\\ &= 1 - \mathbf{p}_k^H(\theta,\phi)\mathbf{E}_{n_1}^*\mathbf{E}_{n_1}^T\mathbf{p}_k(\theta,\phi). \quad (C.2)\end{aligned}$$

Because the second term $\mathbf{p}_k^H(\theta,\phi)\mathbf{E}_{n_1}^*\mathbf{E}_{n_1}^T\mathbf{p}_k(\theta,\phi) = \|\mathbf{E}_{n_1}^T\mathbf{p}_k(\theta,\phi)\|^2 = \|\mathbf{p}_k^H(\theta,\phi)\mathbf{E}_{n_1}^*\|^2$ in the right-hand side of (C.2) does not assume a negative value, the eigenvalues of $\mathbf{T}(\theta,\phi)$ are equal to or less than one. Clearly, we have $\lambda_k(\theta,\phi) = 1$ if and only if $\|\mathbf{p}_k^H(\theta,\phi)\mathbf{E}_{n_1}^*\|^2 = \|\mathbf{g}_k^H(\theta,\phi)\mathbf{E}_{s_1}^H\Psi(\theta,\phi)\mathbf{E}_{n_1}^*\|^2 = 0$.

## References


[1] D. Astély, B. Ottersten, The effects of local scattering on direction of arrival estimation with MUSIC, IEEE Trans. Signal Process. 47 (December 1999) 3220–3234.

[2] D. Asztély, B. Ottersten, A.L. Swindlehurst, Generalized array manifold model for wireless communication channels with local scattering, IEE Proc. - Radar, Sonar, Navig. 145 (February 1998) 51–57.

[3] M. Bengtsson, B. Ottersten, Low-complexity estimators for distributed sources, IEEE Trans. Signal Process. 48 (August 2000) 2185–2194.

[4] M. Bengtsson, B. Ottersten, A generalization of weighted subspace fitting to full-rank models, IEEE Trans. Signal Process. 49 (May 2001) 1002–1012.

[5] O. Besson, P. Stoica, Decoupled estimation of DOA and angular spread for a spatially distributed source, IEEE Trans. Signal Process. 48 (July 2000) 1872–1882.

[6] C.T. Chen, Linear System Theory and Design, Saunders College Publishing, Orlando, FL, 1984.

[7] B.H. Fleury, First- and second-order characterization of direction dispersion and space selectivity in the radio channel, IEEE Trans. Inform. Theory 46 (September 2000) 2027–2044.

[8] J. Fuhl, A.F. Molisch, E. Bonek, Unified channel model for mobile radio systems with smart antenna, IEE Proc. - Radar, Sonar, Navig. 145 (February 1998) 32–41.

[9] L.C. Godara, Handbook of Antennas in Wireless Communications, CRC Press, New York, NY, 2001.

[10] J. Goldberg, H. Messer, Inherent limitations in the localization of a coherently scattered source, IEEE Trans. Signal Process. 46 (December 1998) 3441–3444.

[11] I.S. Gradshteyn, I.M. Ryzhik, Table of Integrals, Series, and Products, Academic Press, Orlando, FL, 1980.

[12] A. Kavak, M. Torlak, W.J. Vogel, G. Xu, Vector channels for smart antennas-measurements, statistical modeling, and directional properties in outdoor environments, IEEE Trans. Microwave Theory Technol. 48 (June 2000) 930–937.

[13] S.C. Kim, I. Song, S. Yoon, S.R. Park, DOA estimation of angle-perturbed sources for wireless mobile communications, IEICE Trans. Comm. E83B (November 2000) 2537–2541.

[14] S.R. Lee, M.S. Choi, M.W. Bang, I. Song, A three-dimensional distributed source modeling and direction of arrival estimation using two linear array, IEICE Trans. Fund. E86A (January 2003) 206–214.

[15] S.R. Lee, I. Song, Y.U. Lee, T. Chang, H.M. Kim, Estimation of two-dimensional DOA under a distributed source model and some simulation results, IEICE Trans. Fund. E79A (September 1996) 1475–1485.
[16] Y.U. Lee, J. Choi, I. Song, S.R. Lee, Distributed source modeling and direction-of-arrival estimation techniques, IEEE Trans. Signal Process. 45 (April 1997) 960–969.
[17] Y.U. Lee, S.R. Lee, H.M. Kim, I. Song, Estimation of direction of arrival for angle-perturbed sources, IEICE Trans. Fund. E80A (January 1997) 109–117.
[18] Y. Meng, P. Stoica, K.M. Wong, Estimation of the directions of arrival of spatially dispersed signals in array processing, IEE Proc.-Radar, Sonar, Navig. 143 (February 1996) 1–9.
[19] K.I. Pedersen, P.E. Mogensen, B.H. Fleury, A stochastic model of the temporal and azimuthal dispersion seen at the base station in outdoor propagation environments, IEEE Trans. Veh. Technol. 49 (March 2000) 437–447.
[20] R. Raich, J. Goldberg, H. Messor, Bearing estimation for a distributed source: modeling, inherent accuracy limitations and algorithms, IEEE Trans. Signal Process. 48 (February 2000) 429–441.
[21] R. Roy, T. Kailath, ESPRIT—Estimation of signal parameters via rotational invariance techniques, IEEE Trans. Acoust. Speech Signal Process. 37 (July 1989) 984–995.
[22] S. Shahbazpanahi, S. Valaee, M.H. Bastani, Distributed source localization using ESPRIT algorithm, IEEE Trans. Signal Process. 49 (October 2001) 2169–2178.
[23] I. Song, J. Bae, S.Y. Kim, Advanced Theory of Signal Detection, Springer, Berlin, Germany, 2002.
[24] T. Trump, B. Ottersten, Estimation of nominal direction of arrival and angular spread using an array of sensors, Signal Processing 50 (April 1996) 57–69.
[25] S. Valaee, B. Champagne, P. Kabal, Parametric localization of distributed sources, IEEE Trans. Signal Process. 43 (September 1995) 2144–2153.
[26] Q. Wan, Y.-N. Peng, Low-complexity estimator for four-dimensional parameters under a reparameterized distributed source model, IEE Proc. - Radar, Sonar, Navig. 148 (December 2001) 313–317.
[27] P. Zetterberg, B. Ottersten, The spectrum efficiency of a base station antenna array system for spatially selective transmission, IEEE Trans. Veh. Technol. 44 (August 1995) 651–660.